



Semnan University

# Progress in Engineering Thermodynamics and Kinetics Journal

Journal homepage: <https://jpetk.semnan.ac.ir/>

## Research Article

# Investigation of $\gamma'$ Precipitates Growth Kinetics in CMSX-4 Based on the Johnson-Mehl-Avrami Model

Sana Rabbani Fard <sup>a \*</sup> , Masumeh Seifollahi <sup>a</sup> , seyed Mahdi Abbasi <sup>a</sup> , Adly AKhondzadeh <sup>a</sup>

<sup>a</sup> Faculty of materials and manufacturing technologies, Malek Ashtar University of Technology, Tehran, Iran

\*corresponding author : [m\\_seifollahi@mut.ac.ir](mailto:m_seifollahi@mut.ac.ir)

## ARTICLE INFO

### Article history:

Received: 202\*-\*\*-\*\*

Revised: 202\*-\*\*-\*\*

Accepted: 202\*-\*\*-\*\*

### Keywords:

CMSX-4 superalloy;

Aging;

 $\gamma'$  Growth Kinetics;

JMAK Model;

## ABSTRACT

CMSX-4 is a second-generation single-crystal nickel-based superalloy. Through aging heat treatments, the characteristics of  $\gamma'$  precipitates, including their size, volume fraction, and morphology, can be controlled in this alloy. Therefore, the main goal of this research is to investigate the effect of aging temperatures (800-1140 °C) and times (1-24 h) on the kinetics of  $\gamma'$  precipitate formation and growth. As the aging temperature increases, the morphology changes from an irregular shape to a cubic one. The most regular cubic morphology is observed at 900 °C. Due to the competition between diffusion and matrix supersaturation, the volume fraction of precipitates initially increases and then decreases with increasing temperature and time. Kinetic studies of  $\gamma'$  precipitate growth and formation using the Johnson –Mehl - Avrami method show that, the rate of transformation and growth of  $\gamma'$  precipitates increases with increasing aging temperature. The average value for the Avrami exponent (n) is approximately 4 in the range of 835-900 °C, which indicates regular and cubic growth of  $\gamma'$  precipitates within this temperature range. Based on this model, a TTP diagram was plotted for CMSX-4. The nose of TTP curve, indicating the optimal conditions for  $\gamma'$  phase formation, which is obtained at approximately 850 °C.

© 2024 The Author(s). Progress in Engineering Thermodynamics and Kinetics Journal published by Semnan University Press.

\* Corresponding author.

E-mail address: [m\\_seifollahi@mut.ac.ir](mailto:m_seifollahi@mut.ac.ir)

## Cite this article as:

Sana Rabbani Fard, Masumeh Seifollahi, Seyed Mahdi Abbasi, Adly AKhondzadeh (2025). Investigation of  $\gamma'$  Precipitates Growth Kinetics in CMSX-4 Based on the Johnson-Mehl-Avrami Model, . Progress in Engineering Thermodynamics and Kinetics. <https://doi.org/>

## 1. Introduction

CMSX-4<sup>1</sup> is a second-generation single-crystal nickel-based superalloy. It is used for gas turbine blade applications due to its desirable properties, including high creep and mechanical/thermal fatigue strength, good phase stability, high resistance to hot corrosion and oxidation [1]. These properties result from its microstructure, which contains a strengthening  $\gamma'$ <sup>2</sup> phase uniformly distributed with a cubic morphology in the matrix. This alloy is subjected to working conditions or heat treatments at temperatures close to the  $\gamma'$  solvus. Therefore, evaluating the characteristics of the  $\gamma'$  phase and its formation and growth kinetics is highly important to achieve the desired mechanical properties. Heat treatment of single-crystal components typically includes a solution annealing stage followed by aging. The purpose of aging is to achieve a uniform distribution of  $\gamma'$  precipitates in terms of size, volume fraction, and morphology. As aging temperature and time increase, the size of  $\gamma'$  particles increases [2-4]. The coarsening of  $\gamma'$  particles is due to the Gibbs-Thomson effect. According to this phenomenon, solute atoms flow from the surface of secondary  $\gamma'$  particles to the matrix and from the matrix towards primary  $\gamma'$  particles, due to the existing concentration gradient. During this process, the average radius of  $\gamma'$  particles increases, while their number decreases, thus reducing the surface free energy of the system. In other words, secondary  $\gamma'$  particles have a higher interfacial curvature and thus a higher concentration of solute around them. Primary  $\gamma'$  particles have less excess energy due to lower curvature and have a lower concentration of solute around them. This causes a concentration gradient from the secondary  $\gamma'$  to the primary  $\gamma'$ , leading to the dissolution of some larger (primary  $\gamma'$ ) precipitates. The Gibbs-Thomson effect is especially important in precipitation systems; it is the driving force for coarsening and coalescence of  $\gamma'$  precipitates at high temperatures [5, 6].

The kinetics of  $\gamma'$  precipitate formation and growth are estimated using the Johnson-Mehl-Avrami (JMAK) model. According to this model, the change in volume fraction of a phase over time, or in other words, the rate of transformation, is obtained by Equation (1) [7-10].

Equation 1: 
$$f = 1 - \exp(-kt^n)$$

In this equation, 'f' represents the volume fraction of the phase and 't' is time. 'k' is the rate constant depending on the nucleation and growth rate. 'n' is the time exponent which indicates the type of nucleation. Parameters 'n' and 'k' are material and temperature-dependent parameters [11] which are used to determine the kinetics of isothermal reactions. Based on previous studies [11-14] and the average value of the Avrami exponent (n), the morphology

---

<sup>1</sup> Cannon Muskegon Single Crystal

<sup>2</sup> Gamma prime

and growth pattern of the precipitates can be determined. This model has also been used for superalloys to analyze the kinetic behavior of precipitates and to plot TTP<sup>3</sup> curves [7, 15]. For example, in the report by Masoumi et al. [13], the average value of the Avrami exponent obtained (n) between 1.5 and 2.3 that indicates irregular and spherical growth.

Lapin et al. [16] investigated the effect of aging time and temperature on the growth kinetics of  $\gamma'$  in CMSX-4 using the LSW<sup>4</sup> method. According to their study, the growth kinetics of  $\gamma'$  precipitates follows a third-power law, which is controlled by volume diffusion of alloying elements in the  $\gamma$  matrix.

Matan et al. [17] also investigated the rafting kinetics of the CMSX-4 superalloy under creep conditions and heat treatment. According to their findings, for smaller values, thermal strain-induced rafting occurs very slowly. The magnitude of the thermal strain reduces the  $\gamma/\gamma'$  interfacial coherency and reduces surface stresses.

Due to the lack of investigation into the kinetics of transformation and growth of  $\gamma'$  in the literature, the present study investigates the kinetics of transformation and growth of  $\gamma'$  in CMSX-4 using the Johnson-Mehl-Avrami method. Furthermore, due to the importance of TTP diagrams, this curve was plotted for 1%, 50%, and 99% volume fraction of  $\gamma'$  precipitates.

## 2. Materials and Methods

CMSX-4, with the chemical composition shown in Table 1, was melted and cast in a VIM furnace and then grown as a single crystal in a laboratory Bridgman furnace. The chemical composition was determined using quantometry method (Spectro2004) and inductively coupled plasma mass spectroscopy (ICP-MS). The alloy underwent a four-stage solution annealing heat treatment cycle, according to standard method which published by **Cannon Muskegon Corp.**, as follows:

1277°C/1h/(0.33°C/min) + 1287°C/1h/(0.33°C/min) + 1297°C/1h/(0.33°C/min) + 1307°C/2h/AC

Then, the samples were aged at temperatures of 800-1000°C for times of 1, 3, 9, and 25 hours. After sanding and polishing, the surfaces of the samples were etched using a solution of HCl and HNO<sub>3</sub> in a 1:1 ratio [18]. The microstructure was examined using a scanning electron microscope (MIRA3 TESCAN), and images were analyzed using ImageJ analysis software.

<sup>3</sup> Time Temperature Transformation

<sup>4</sup> Lifshitz-Slyozov-Wagner

Table 1: Chemical Composition of the CMSX-4 Superalloy (wt%).

Element	Ni	Al	Ti	Cr	Co	Mo	Ta	W	Re	Hf
Results	Bal	6.5	0.98	5.6	9.59	7.0	6.6	6.6	3.05	0.01

### 3. Results and Discussion

Figure 1 shows the microstructure of  $\gamma'$  precipitates in CMSX-4 superalloy after aging. The volume fraction and size of the  $\gamma'$  were calculated, and the results are plotted in the graph of Figure 2. As can be seen in Figure 1, below 870 °C, with increasing time, the morphology of  $\gamma'$  changes from an irregular and shapeless state to a regular cubic morphology. The morphology becomes significantly regularly cubic shape at 835 °C/25 hr aging. According to Figure 2, the size of  $\gamma'$  at 800 °C and 835 °C initially increase slowly with increasing aging time, which is due to the low diffusion rate of solute atoms in the matrix. After 20 hours, a significant increase in the size of  $\gamma'$  is observed. At 870 °C, the  $\gamma'$  precipitates grow significantly with increasing time above 3 hours, and they maintain their cubic morphology up to 25 hours aging. Figure 1 also shows at 900 °C/3hr, some of the  $\gamma'$  precipitates with irregular morphology, take on a regular cubic shape with increasing time to 10 hr, but their size does not change up to 25 hr. Also, according to Figure 1, it can be stated that at 1000 °C, with increasing time, the size of the  $\gamma'$  increases, and their morphology changes from a regular cubic to an irregular, shapeless morphology.  $\gamma'$  size increasing is due to the coalescence of the  $\gamma'$  precipitates at higher times, in order to reduce the surface energy and diffusion rate increasing of solute atoms. So, it is necessary to also examine the  $\gamma'$  precipitates of the alloy from to determine the optimal heat treatment conditions. As is evident in Figure 1, the complete cubic morphology corresponds to 900 °C, which is more regular than other temperatures. Therefore, by calculating the average size of  $\gamma'$  precipitates at this temperature, it can be argued that the appropriate morphology for the CMSX-4 alloy is a cubic morphology with an average size of 478 nm. Considering that the morphology and regularity are suitable for this temperature compared to others so the optimum range of aging is expected to be around 900 °C. Also, above 900 °C are close to  $\gamma'$  solvus temperature, so, in addition to growth, these precipitates also dissolve into the matrix. The size of the  $\gamma'$  precipitates increases as the fine precipitates coalesce. Then, given that the structure is cubic, the precipitates gradually begin to change morphology from cubic to spherical in order to reduce their surface energy.

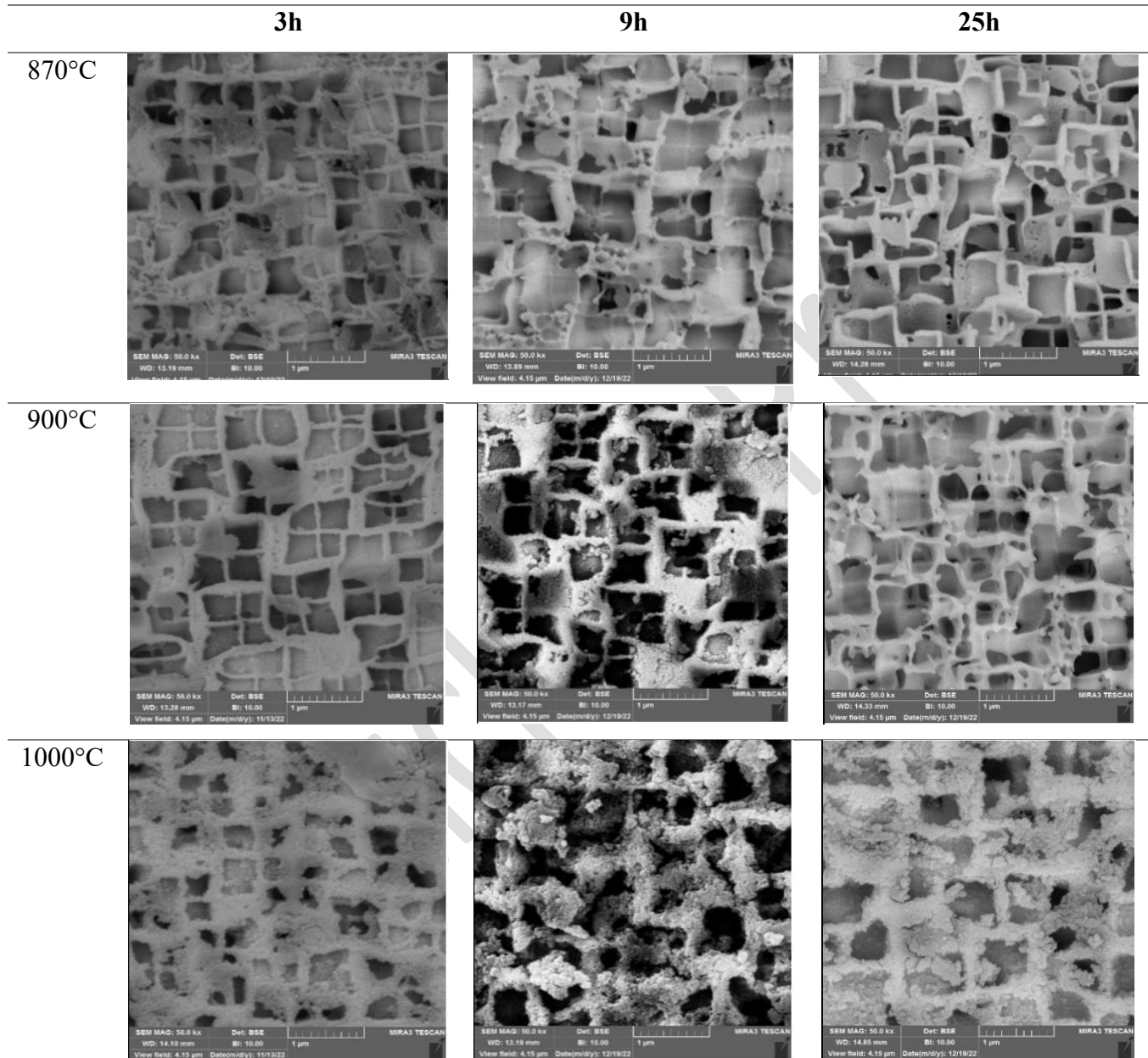


Figure 1: SEM micrograph of CMSX4 Microstructure after aging at 870°C, 900°C and 1000°C for 3, 9 and 25 hours.

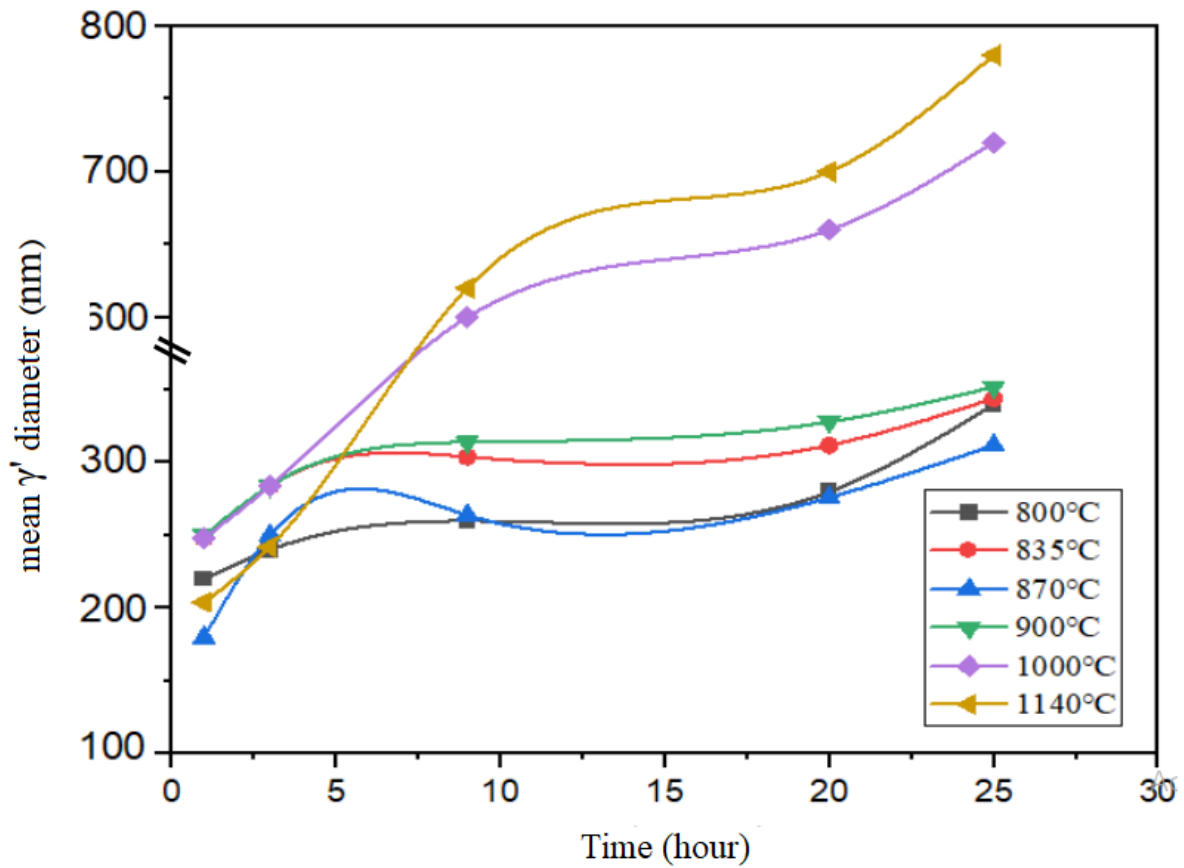


Figure 2: Size of  $\gamma'$  precipitates based on aging time at different aging temperatures.

Figure 3 also illustrates the  $\gamma'$  volume fraction versus aging temperatures and times. As seen in the graphs, the volume fraction of the precipitates increases with a relatively low slope up to 20 hours at 800°C and 835°C, and after that, the volume fraction remains approximately constant. However, at 870°C, the volume fraction increase steeply, with the value rising suddenly from about 40% at 1 hr to around 55%, and again, at 9 hours, the volume fraction reaches about 67%. After that, the volume fraction remains nearly constant with further increases time. Time increasing only leads to the growth and formation of the cubic morphology of  $\gamma'$ . At 900°C,  $\gamma'$  volume fraction increases with a relatively low slope until 25 hr, such that the volume fraction rises from about 52% after 3 hr to approximately 67 percent after 25 hr. At 1000°C, the volume fraction initially increases with aging, but at longer aging times, the volume fraction decreases; in other words, the increase in aging time leads to the growth and dissolution of the  $\gamma'$  precipitates in the matrix.

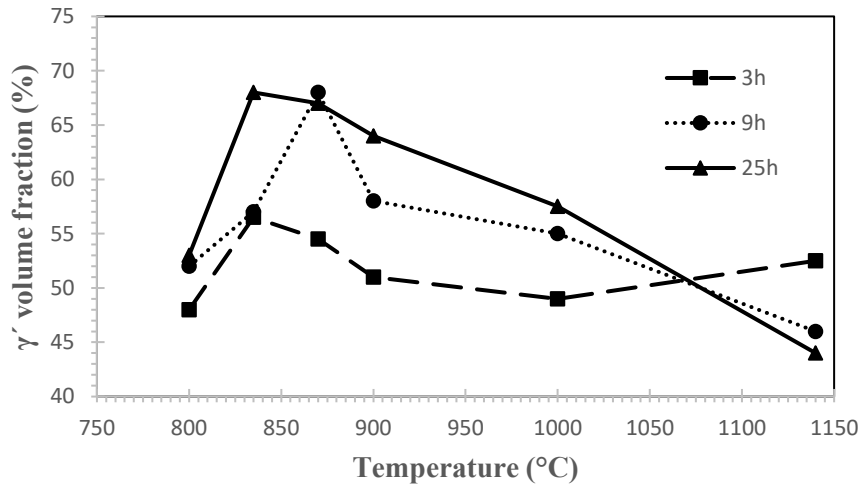


Figure 3: Graph of the effect of aging temperatures and times on volume fraction of  $\gamma'$  precipitates in the CMSX-4 superalloy.

Based on the results obtained for the volume fraction of  $\gamma'$  precipitates at different conditions, according to relation 1, the curve of  $\ln \ln(1/(1-f))$  versus  $\ln t$ , based on the Johnson-Mehl-Avrami model [19, 20] for the CMSX-4 alloy aged at 800-1000 °C, is plotted in Figure 4. ( $t$  is time and  $f$  is the volume fraction of the  $\gamma'$  phase). From the slopes of the lines, the value of  $n$  (Avrami exponent) can be determined, and from their intercepts,  $k$  (time coefficient in the mentioned equation) can be obtained. As seen in Figure 3, with increasing temperature,  $n$  initially decreases and then shows a slight increase. This is because, with increasing temperature, the conditions for phase transformation become more favorable due to enhanced diffusion, leading to an increased fraction of transformed material and consequently an increase in  $n$ . The values of  $n$  and  $k$  are presented in Table 2. The exponent  $n$  (Avrami exponent) indicating the type and manner of growth of  $\gamma'$ . An  $n$  value between 3 and 4 indicates regular and cubic growth of the  $\gamma'$ , while values less than 3, indicate irregular and spherical growth of the  $\gamma'$  [11, 12]. As the difference of  $n$  from these values increases, the  $\gamma'$  grows irregularly. As shown in Figure 1, the growth of the  $\gamma'$  at 835, 870, and 900 °C is cubic, while at 800 and 1000 °C, it is irregular and lacks a specific shape. The average value of  $n$  obtained in the present study is approximately 4, indicating cubic growth of the  $\gamma'$  precipitates in the CMSX-4 alloy.

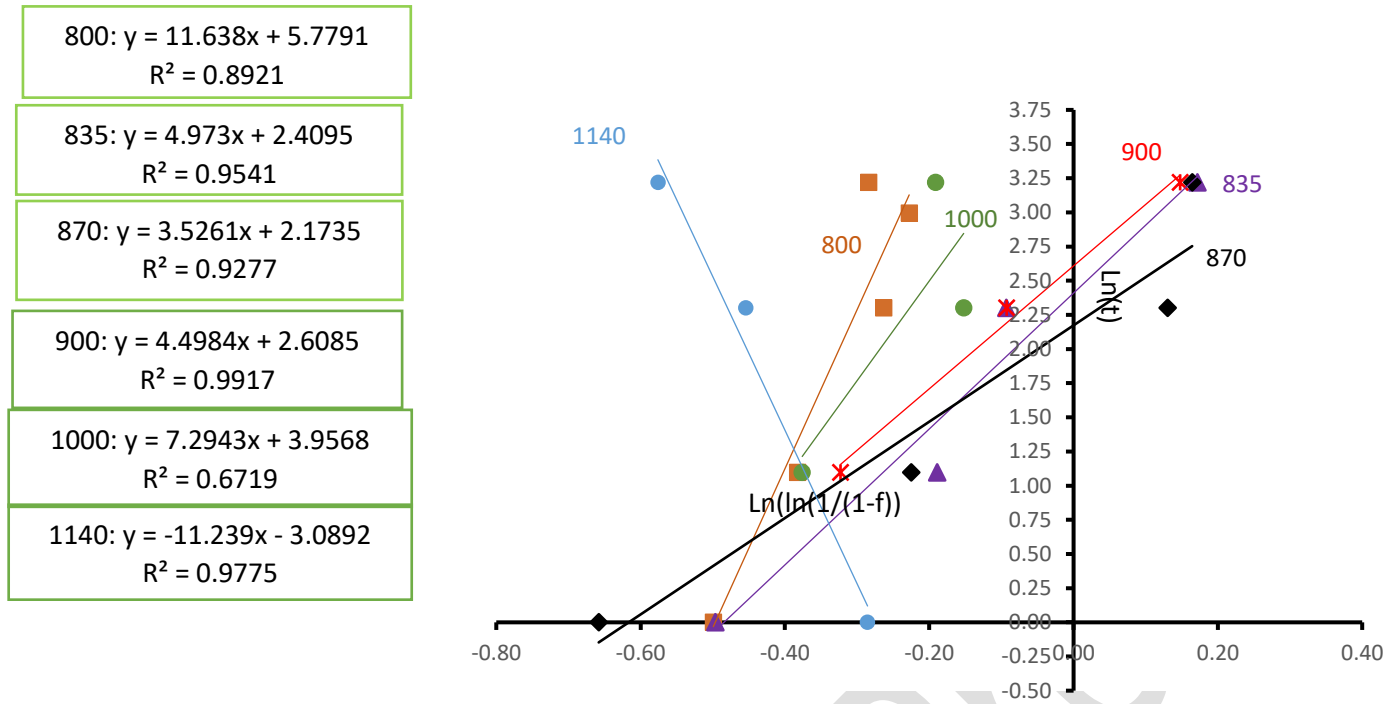


Figure 4: Curve of  $\ln(\ln(1/(1-f)))$  versus  $\ln(t)$  for the CMSX-4 alloy aged at different temperatures.

Table 2: Values of  $n$  and  $k$  for the CMSX-4 alloy aged at different temperatures.

$n$	$K$	Temperatures (°C)
4.66	0.0216	<b>800</b>
4.88	0.0955	<b>835</b>
3.45	0.1179	<b>870</b>
3.94	0.0870	<b>900</b>
3.46	0.0731	<b>1000</b>

The negative slope at a 1140°C, as seen in Figure 4, indicates that with an increase in aging time at this temperature, the  $\gamma'$  begin to dissolve in the matrix. The changes in the creep strength are due to kinetics that are significantly influenced by aging temperatures, and according to the studies by Kormir and colleagues [11], the Johnson-Mehl-Avrami model should be considered as a qualitative nature for the aging behavior of CMSX-4.

The equation for the formation rate of the  $\gamma'$  phase at different temperatures is presented in Table 3 and plotted in Figure 5. As observed in Figure 5, with increasing temperature, the formation rate and the fraction of  $\gamma'$  precipitates increase and the amount of the  $\gamma'$  phase reaches its maximum value in shorter times. This trend is observed up to 835 °C, but at 870 °C and 900 °C, the formation rate decreases compared to other temperatures. Additionally, at 1140 °C,



given that the slope of the graph is negative, it can be stated that with increasing aging time at 1140 °C, the  $\gamma'$  begin to dissolve. It is confirmed in [21]

Furthermore, the TTP curve for the initiation, 50% and the completion of  $\gamma'$  phase formation in the CMSX-4, derived from the formation rate equations, is plotted in Figure 6. These curves are drawn by substituting values of 0.01, 0.5, and 0.99 for  $f$  in the formation rate equations. As seen in Figure 6, it can be stated that based on the formation and transformation rate equation obtained from the Johnson-Mehl-Avrami method which presented in Table 3, the shortest time required for the formation of 1%  $\gamma'$  corresponds to 870 °C over a duration of 32 minutes of aging. Additionally, after aging for 94 minutes at 870 °C, approximately 50% of the  $\gamma'$  phase precipitate is formed. The tip of the TTP, which represents the optimal thermal and temporal conditions for the formation of the  $\gamma'$  in terms of diffusion and supersaturation of the matrix, is achieved at around 850 °C. Above the tip temperature, supersaturation decreases, and below the tip one, the conditions for diffusion are not optimal [22]. Therefore, it can be stated that the formation rate equations obtained from the Johnson-Mehl-Avrami method are suitable for the CMSX-4 alloy, and through these equations, the formation times for different volume fractions of  $\gamma'$  can be predicted. It is also evident from the TTP diagram that at 1140 °C, the  $\gamma'$  precipitates begin to dissolve in the  $\gamma$  matrix phase.

Table 3: Rate equation for the formation of the  $\gamma'$  phase for the CMSX-4 alloy aged at different temperatures.

equation of formation rate	Temperatures (°C)
$F=1-\exp(-0.0216t^{4.66})$	<b>800</b>
$F=1-\exp(-0.0955t^{4.88})$	<b>835</b>
$F=1-\exp(-0.1179t^{3.45})$	<b>870</b>
$F=1-\exp(-0.0870t^{3.94})$	<b>900</b>
$F=1-\exp(-0.0371t^{3.46})$	<b>1000</b>

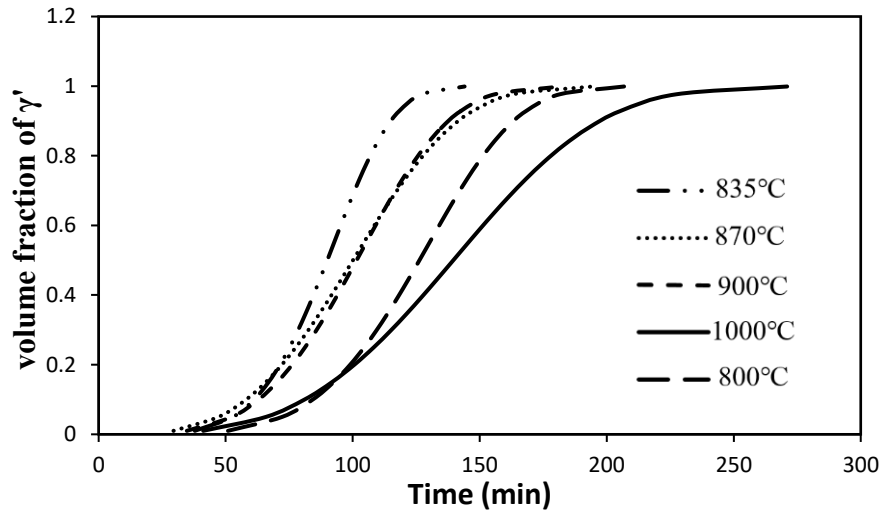


Figure 5: Curve of the volume fraction of  $\gamma'$  precipitate formation versus time for the CMSX-4 alloy aged at different temperatures.

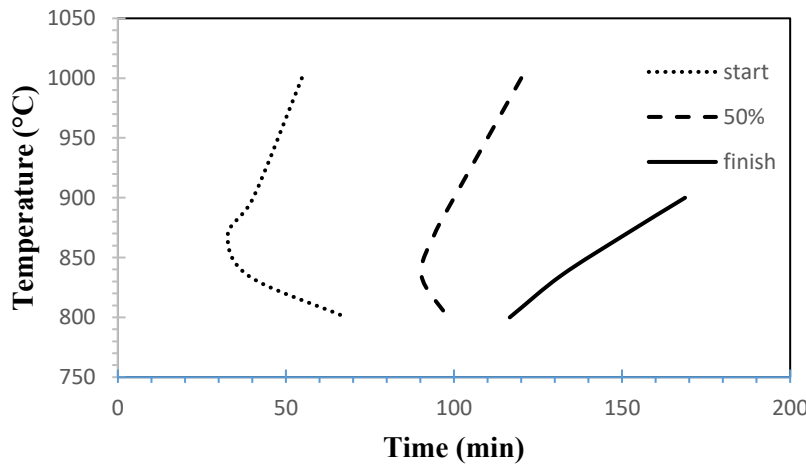


Figure 6: TTP diagram plotted for the  $\gamma'$  phase based on the Johnson-Mellor model.

#### Conclusion:

- 1- Based on microstructural studies and kinetic equations, the TTP curve for the precipitation of  $\gamma'$  in the CMSX-4 alloy was plotted.
- 2- The average value for the Avrami exponent ( $n$ ) in the range of 900-835 °C is approximately 4, indicating the regular and cubic growth of  $\gamma'$  precipitates within this temperature range.
- 3- According to the microstructural and kinetic studies based on the Johnson-Mehl-Avrami method, the time required for the formation of  $\gamma'$  at 870 °C is 32 minutes, which is the minimum time needed for the formation of 50% of the  $\gamma'$  phase precipitates. The subsequent

time relates to the aging at 900 °C; therefore, conducting the aging process at these two temperatures is favorable from a kinetic perspective.

- 4- The tip of the TTP curve, which indicates the optimal temperature and time conditions for the formation of the  $\gamma'$  phase, was obtained at approximately 850 °C.

## References

1. Ali Jadidi, A. , Abbasi, S.M. Seifollahi, M. (2024). microstructural evolution of cmsx-4 single crystal superalloy with varying distance from the chill plate, *Journal of Manufacturing Innovations 1*, 28-35.doi: 10.22055/jomi.2024.46962.1019.
2. Szczotok, A. (2016) Effect of two different solutionizing heat treatments on the microstructure of the CMSX-4 Ni-based superalloy. in Solid State Phenomena. Trans Tech Publ.
3. Condruz, M.R., et al.,(2018) Homogenization heat treatment and segregation analysis of equiaxed CMSX-4 superalloy for gas turbine components. *Journal of Thermal Analysis and Calorimetry*, 134(1): p. 443-453.
4. Wahlmann, B., et al., (2019) Growth and coarsening kinetics of gamma prime precipitates in CMSX-4 under simulated additive manufacturing conditions. *Acta Materialia*, 180,. 84-96.
5. Baldan a. (2002) Progress in Ostwald ripening theories and their applications in nickel-base super alloys. *Journal of Mater Science.*,37, 2379–405.
6. Ivanskii B V., Vengrenovich RD. (2016) To the theory of Ostwald ripening in metallic alloys. *Physics of Metals and Metallography*.117, 756–65.
7. M. Seifollahi, P. Sahrapour, S. M. Abbasi, Sh. Kheirandish, S. H. Razavi, (2018) Mathematical-Thermodynamic Prediction and Kinetics of Eta Phase Formation in Fe–Ni-Based Superalloys, *Transactions of Indian Institute of Metals*, 71(1),147–152.
8. Christian JW. (1975) The Theory of Transformations in Metals and Alloys. I. Equilib Gen Kinet theory.
9. Rafiei M, Mirzadeh H, Malekan M, Sohrabi MJ. (2019) Homogenization kinetics of a typical nickel-based superalloy. *Journal of Alloys and Compound*,doi:10.1016/j.jallcom.2019.04.147
10. Naghizadeh M, Mirzadeh H. (2018) Modeling the kinetics of deformation-induced martensitic transformation in AISI 316 metastable austenitic stainless steel. *Vacuum*. 157, 243–8.
11. Cormier J, Gadaud P, Czaplicki M, Zhang RY, Dong HB, Smith TM, (2021) In-situ determination of precipitation kinetics during heat treatment of superalloy 718. *Metallurgy and*

*Materials Transactions A*, 52:500–11.

12. Rafiei M, Mirzadeh H, Malekan M. (2020) Precipitation kinetics of  $\gamma''$  phase and its mechanism in a Nb-bearing nickel-based superalloy during aging, *Vacuum*, 178, 109456.
13. Masoumi F, Shahriari D, Jahazi M, Cormier J, Devaux A. (2016) Kinetics and Mechanisms of  $\gamma'$  Reprecipitation in a Ni-based Superalloy. *Scientific Reports*, 28650, doi:10.1038/srep28650
14. Jia L, Cui H, Yang S, Lv S, Xie X. (2023) As-cast microstructure and homogenization kinetics of a typical hard-to-deform Ni-base superalloy. *Journal of Materials Research Technology*. 23:5368–81. doi:10.1016/j.jmrt.2023.01.150
15. M. Seifollahi, Sh. Kheirandish, S. H. Razavi, S. M. Abbasi, (2013) The precipitation of  $\eta$  phase in an Fe-Ni based superalloy with different Ti/Al ratios, *international journal of materials research*. 104, 344-350.
16. Lapin J, Gebura M, Pelachova T, Nazmy M. (2008) Coarsening kinetics of cuboidal  $\gamma$  precipitates in single crystal nickel base superalloy CMSX-4. *Kovove Materialy*. 46:313–22.
17. Matan N, Cox DC, Rae CMF, Reed RC. (1999) On the kinetics of rafting in CMSX-4 superalloy single crystals. *Acta Materialia*. 47, 2031–45.
18. Szczotok, A. Reichel, H. (2020). Methodology for revealing the phases and microstructural constituents of the cmsx-4 nickel-based superalloy implicating their computer-aided detection for image analysis. *Materials*, 13, 341; doi:10.3390/ma13020341.
19. Raghavan, V. (19987) Solid state phase transformations. PHI Learning Pvt. Ltd
20. Christian, J.W. (1975) The Theory of Transformations in Metals and Alloys. I. Equilibrium and general kinetic theory. 1975.
21. Li, D. Li, G. Wei, X. Ma, B. Huang, C. Chen, W. Zhao, P. Wang, L. Zeng, Q.(2024) Long-term aging behavior and mechanism of CMSX-4 nickel-based single crystal superalloy at 950 °C and 1050 °C, *Journal of Alloys and Compounds*, 1004, 175763, doi:10.1016/j.jallcom.2024.175763.
22. Uddagiri, M., Shchyglo, O., Steinbach, I. (2024) Solidification of the Ni-based superalloy CMSX-4 simulated with full complexity in 3-dimensions. *Progress Additive Manufacturing*. 9, 1185–1196 (2024) doi: 10.1007/s40964-023-00513-9